NASA

Technical Memorandum **85099**

EVIDENCE FOR VARIABILITY OF THE HARD X-RAY FEATURE IN THE HERCULES X-1 ENERGY SPECTRUM

J. Tueller, T.L. Cline, B.J. Teegarden, W.S. Paciesas, D. Boclet, Ph. Durouchoux, J.M. Hameury, N. Prantzos, and R.C. Haymes

August 1983

National Aeronautics and
Space Administration

Goddard Space Flight Center
Greenbelt, Maryland 20771

I. INTRODUCTION

The X-ray source Her X-1 was first discovered by Tananbaum et al. (1972), and the optical companion star HZ Her was identified by Liller (1972) and Bahcall and Bahcall (1972). At least three different periodicities have been observed in the X-ray emission; 1. a period of 1.24 s associated with the neutron star rotation period, 2. a 1.7-day period associated with eclipsing by the companion star, 3. a 35-day cycle associated with the precession of the accretion disk. For a summary of the X-ray measurements of Her X-1 see McCray et al. (1982).

A hard X-ray feature in the Her X-1 spectrum was first reported by the MPI/AIT group (Trümper et al., 1978). They observed a feature which was consistent with a narrow (< 13 keV) emission line at 58 keV with an intensity of $3.4 \cdot 10^{-3}$ ph/cm^2·s. Since then there have been a number of confirmations of these results by experiments of similar resolution (Gruber et al., 1980; Voges et al., 1982; Sheepmaker et al., 1981; Ubertini et al., 1981). While these later results have been interpreted as being inconsistent with a narrow line, the minimum line width was in every case significantly less than the resolution of the experiments. For summaries of these measurements see Staubert et al. (1981).

The MPI/AIT group interpreted this unexpected observation of a hard X-ray feature as a cyclotron emission line from the high magnetic fields near the pole of the neutron star. In the original measurement they also observed a feature at 120 keV which they suggested could be the second harmonic of the primary cyclotron line. This feature has not been confirmed in later measurements. Further considerations of both the theory of cyclotron lines and the observational data have shown that the feature could be explained equally well as an absorption line. The observation of a second harmonic

ABSTRACT

The hard X-ray spectrum of HER X-1 was measured for the first time with a high resolution (1.4 keV FWHM) germanium spectrometer. The observation was performed near the peak of the on-state in the 35-day cycle and the 1.24 s pulsations were observed between the energies of 20 keV and 70 keV. We confirm the observations of a hard X-ray feature in the pulsed energy spectrum which has been associated with a cyclotron line (Trumper et al., 1978). The feature corresponds to an excess of 7.5 sigma over the low energy continuum. Smooth continuum models are poor fits to the entire energy range (chance probabilities of 2 percent or less). The best fit energies are 35 keV for an absorption line and 39 keV for an emission line. These are significantly lower energies than those derived from previous experiments. A direct comparison of our data with the results of the MPI/AIT group shows statistically significant variations which strongly suggest variability in the source. We see no evidence for a second harmonic emission line around 120 keV (upper limit for a narrow line, $2 \cdot 10^{-4}$ ph/cm^2·s).

subject headings: stars: individual (Her X-1) -
X-rays: binaries - X-rays:spectra

I. INTRODUCTION

The X-ray source Her X-1 was first discovered by Tananbaum et al. (1972), and the optical companion star HZ Her was identified by Liller (1972) and Bahcall and Bahcall (1972). At least three different periodicities have been observed in the X-ray emission; 1. a period of 1.24 s associated with the neutron star rotation period, 2. a 1.7-day period associated with eclipsing by the companion star, 3. a 35-day cycle associated with the precession of the accretion disk. For a summary of the X-ray measurements of Her X-1 see McCray et al. (1982).

A hard X-ray feature in the Her X-1 spectrum was first reported by the MPI/AIT group (Trümper et al., 1978). They observed a feature which was consistent with a narrow (< 13 keV) emission line at 58 keV with an intensity of $3.4 \cdot 10^{-3}$ ph/cm^2·s. Since then there have been a number of confirmations of these results by experiments of similar resolution (Gruber et al., 1980; Voges et al., 1982; Sheepmaker et al., 1981; Ubertini et al., 1981). While these later results have been interpreted as being inconsistent with a narrow line, the minimum line width was in every case significantly less than the resolution of the experiments. For summaries of these measurements see Staubert et al. (1981).

The MPI/AIT group interpreted this unexpected observation of a hard X-ray feature as a cyclotron emission line from the high magnetic fields near the pole of the neutron star. In the original measurement they also observed a feature at 120 keV which they suggested could be the second harmonic of the primary cyclotron line. This feature has not been confirmed in later measurements. Further considerations of both the theory of cyclotron lines and the observational data have shown that the feature could be explained equally well as an absorption line. The observation of a second harmonic

feature would be crucial in distinguishing between these alternatives. For a detailed discussion of the cyclotron line theory see Nagel (1981a, 1981b) and Mészáros et al.(1983). The confirmation of this feature by a high resolution experiment with different systematics is an important new result.

II. INSTRUMENT AND OBSERVATION

The experiment consists of a balloon-borne array of three high-purity planar germanium crystals. The detectors are 1 cm thick and have a combined effective area of 53 cm^2 at 60 keV. The efficiency of these detectors is nearly constant from 20 to 100 keV (the effective range of the Her X-1 measurement) and the energy resolution over this range is independent of energy with a value of 1.4 keV FWHM. Both the resolution and the energy calibration are accurately determined from strong narrow background lines in the flight data. Collimation is provided by a combination of a heavy active shield of NaI and a passive iron collimator to restrict the field-of-view to 5° x 10° FWHM. This combination achieves a very low background continuum (the maximum at 30 keV is $3 \cdot 10^{-4}$ cnts/$cm^2 \cdot s \cdot keV$) which compensates for the relatively small effective area of the primary detectors. The telescope is mounted in an altazimuth pointing system with a pointing accuracy of ~ 1°. For a more detailed description of the experiment, see Paciesas et al. (1982).

The source was observed from 18:30 UT on 1980 September 24 to 3:00 UT the next day. Background was obtained by alternating on-source pointing with off-source pointing every 20-min. (The off-source direction was typically offset in azimuth by 30° or 180° from the source direction.) The orbital phase varied from 0.04 to 0.23 during the observation (Deeter et al. 1981). Because the source was eclipsed during the first source pointing, this interval was not used during the subsequent analysis. The phase of the 35-day ON-OFF cycle

is rather uncertain, but the the level of continuum intensity indicates that it was near the peak of the ON phase. Preliminary results from this observation were published by Tueller et al. (1981).

III. ANALYSIS OF PULSATIONS

Figure 1 shows the average pulsation light curve derived from a summed epoch analysis of the on-source pointings. The number of counts between 20 and 65 keV was accumulated in 32 bins according to the pulse arrival time (quantized in 100 μs intervals), folded at various periods, and corrected for the orbital motion of Her X-1. The light curve shown corresponds to the period which maximizes the χ^2 deviation of the phase bins from the average number of counts for the entire observation. The baricentric period, 1.237791 ± 0.000002 s was derived from a weighted mean of the periods near the peak in the χ^2 distribution. Its uncertainty was determined by a Monte Carlo analysis which included the actual source observing intervals and possible variations in the ideal light curve, as well as statistical fluctuations. The dashed line shows the average number of counts for the same total time from the off-source pointings. The pulsed fraction derived from the data in Figure 1 is 1.01 ± .18. The pulsed fraction was defined as the ratio of the number of counts in the peak (after the presumed phase-independent source counts under the peak are subtracted) divided by the phase-independent counts. We have also examined the light curve in smaller energy bins for variations in the pulsed fraction or pulse shape. No statistically significant variations were observed; however, the data show some indication of a drop in the pulsed fraction below 25 keV which is consistent with the break observed in the energy spectrum at that energy.

IV. SPECTRAL ANALYSIS

One of the primary goals of this experiment is the search for narrow lines in astrophysical sources. Figure 2 shows the results of a search for narrow lines in the pulse spectrum (defined by the phase region labeled PULSE in Figure 1). The solid curve is our three-sigma upper limit on narrow line intensity as a function of energy. This limit was derived from the difference between the counts in a 1.8 keV wide bin and one-third of the counts in two adjacent 2.7 keV bins. The bin width was chosen to optimize the sensitivity to a narrow line. The spectrum was sampled by moving these bins in steps of 0.9 keV through all energies. No fluctuations, positive or negative, with a significance greater than three sigma were observed in the energy range shown. The curve corresponds to the three-sigma upper limit in this difference converted to the intensity of a narrow line at the top of the atmosphere (1.4 KeV FWHM at the detector). The gaps in the solid curve are in the region of strong background lines of 23 keV, 67 keV, and 138 keV; in these regions our sensitivity is greatly reduced due to much higher background and the rapid variation of the background level. Also shown on the figure are three data points that correspond to the derived parameters for a broad emission line feature in our data and those of the MPI/AIT group. Our data show conclusively that this feature cannot be attributed to narrow lines and, further, there is no evidence for any narrow line contribution to the broad features.

Since we have shown that there are no narrow features in the spectrum, we are justified in binning our data in larger energy bins in order to improve the statistical significance of individual data points. Figure 3 shows a spectrum derived for the pulsed data with background subtracted as determined from the off-source pointing intervals. The solid-line histogram represents

the counts spectrum with background subtracted but uncorrected for detector efficiency and atmospheric absorption.

To generate this spectrum, the events from the phase region labeled "PULSE" (Figure 1) in each source observation were converted to a rate by dividing by the total livetime in each source interval (~ 20 min). This is the conventional normalization used in X-ray pulse-phase spectroscopy. A background rate, determined from the sum of 10-minute intervals before and after the source interval, was subtracted. Small corrections were applied for the average collimator transmission and to normalize each interval to the average atmospheric depth of 4.9 gm/cm^2. Finally, the corrected rates from each source interval were summed together to produce the counts spectrum. A model source spectrum with 0.5 keV energy bins was folded with a response matrix to calculate a trial counts spectrum for comparison with the measured spectrum. The response matrix included the effects of atmospheric absorption, full-energy peak response, K-escape, and detector resolution. Fits were performed by adjusting the model parameters to find the values corresponding to the minimum χ^2 deviation between the trial counts spectrum and the measured values. The searches of the model parameter space were performed using a modified version of the CURFIT routine from Bevington (1969). A source photon spectrum was produced by multiplying each measured rate by the ratio of the number of photons in the model spectrum to the number of counts in the trial spectrum.

The source photon data points in Figure 3 were derived using an emission line model. However, because of the fine energy resolution of this experiment, the unfolded source spectrum is nearly independent of the model used, provided that the model can produce a reasonably good fit to the measured count rates. The energy bins in the spectrum are large in comparison

to our energy resolution (1.8 • FWHM for the smallest bins), and the response matrix contains only very small off-diagonal terms due to other effects. Because of this, the procedure used is effectively equivalent to inverting the response matrix and produces a nearly unique source spectrum. This represents an important improvement in the systematic uncertainties in the source spectrum over other experiments lacking our fine energy resolution, where the deconvolved spectrum can be strongly model dependent.

There are several qualitative features which can be easily seen in this spectrum. First, there is a steep decline in the spectrum from 22.5 keV to 37.5 keV, although the lowest energy point (20 keV to 22.5 keV) lies well below the trend of this data. Second, the intensity between 35 and 50 keV is essentially constant. Third, above 50 keV, the spectrum abruptly falls to a level at least 4 to 5 times lower. Above 70 keV only two-sigma upper limits are given. One can derive a rough estimate of the statistical significance of the high-energy excess by subtracting an exponential determined by a fit to the data below 35 keV from the data points above 35 keV. The sum of this difference from 35 to 70 keV has a statistical significance of 7.5 sigma, which is the same as the significance of the feature derived by Trümper et al. (1978).

We have constructed a similar spectrum for the off-pulse phase bin. The statistical uncertainties in this spectrum are substantially larger due to the smaller ratio of source to background. In this spectrum we have a statistically significant source flux only for energies less than 45 keV. An acceptable fit to the off-pulse spectrum can be made with a simple exponential or power-law model. In addition, we have compared the off-pulse spectrum with an emission line model derived from a fit to the pulse spectrum and concluded that this is also an acceptable fit. To make a more model independent

comparison we have normalized the pulse spectrum to the same number of counts as the off-pulse spectrum and calculated the difference. This difference spectrum shows no statistically significant (> 3 sigma) fluctuations. A similar analysis has been performed for 3 equal phase bins dividing up the pulse spectrum. Again, no statistically significant fluctuations were observed. We conclude our data contain no evidence for phase dependence of the Her X-1 spectrum. However, the statistical uncertainties in these results are large and we cannot preclude the kind of phase dependences reported by other observers (Pravdo et al., 1977, 1978, and Gruber et al., 1980).

Table 1 displays the models used to derive fits to the Her X-1 spectrum. Models of the continuum include a power law, an exponential in energy, and a low-energy power law with an exponential cutoff. Each of these models can be used alone to fit the data or in combination with a Gaussian absorption or emission feature. Table 2 displays the best fit parameters derived from these models. The error limits are one sigma (68 percent) joint confidence values derived in the manner of Lampton, Margon and Bowyer (1976). Neither of the smooth continuum fits is a good fit to the data. The chance probability of χ^2 being equal to or greater than the value derived for the power law fit is two percent. For the exponential fit, the probability is less than one percent.

The addition of a break in the model function (low-energy power law with exponential cutoff) does not significantly reduce χ^2. If the energy of the break is allowed to vary, the best fit value is a break near 20 keV (the lower level threshold of this experiment), which is equivalent to eliminating the break from the model. The introduction of an absorption feature produces a good fit to the data with a χ^2 per degree of freedom < 1. The fit produced by the addition of an emission line to the simple exponential is not as good although it still results in an acceptable fit. Most of the difference in χ^2

between the absorption line and emission line model results from the three lowest energy points, which are poorly fit by the simple exponential with a small value of E_0 (the characteristic energy of the exponential). If we allow the break from the power law observed in lower energy X-ray measurements to be at an energy as high as 25 keV, this difference is eliminated. The break allows a very small value of E_0 while maintaining a good fit to the lowest energy data points. In this case, a value of χ^2 is achieved by the emission line model that is equivalent to that of the absorption line model. The break energy is insensitive to the line parameters near the minimum in χ^2 and has not been included as an adjustable parameter in the final emission line model fit. This model is in good agreement with the lowest energy data points, even far from the minimum in χ^2. It must be noted that the inclusion of a break in the continuum model allows acceptable fits to be achieved by the addition of a variety of high-energy excess components other than an emission line. For example, adding a blackbody with a temperature of 8.4 keV yields a $\chi^2 = 13.8$ and adding a high-energy power law tail with a slope of 3.8 yields a $\chi^2 = 19.2$.

The different line parameters derived with the two continuum models reflect the sensitivity of the emission-line fit to the continuum model chosen. A detailed examination of the confidence contours shows that these differences occur predominantly in the limit of higher line intensities and lower line energies. The contours for different continuum models are nearly identical in the region of lower line intensities and higher line energies. This rule holds for the effects of various systematic uncertainties as well.

We have considered the effects of the uncertainty in atmospheric depth and the effect of including small non-diagonal elements in the detector response matrix. In both cases the line parameters are only weakly coupled to

these uncertainties. Fits were performed using values at the extremes of our uncertainty in these two factors, and the resulting changes in the values of the line parameters that minimize χ^2 were always less than $\chi^2_{min} + 1$ error limits. The strongest coupling observed was between atmospheric depth and the continuum intensity in the emission line model. In this case an error of 0.2 gm/cm^2 in the average depth of our observation can shift the χ^2_{min} value of the intensity to around the $\chi^2_{min} + 1$ limit of the unshifted fit. We conclude that these uncertainties do not make a significant contribution to the uncertainty in our results.

Figure 4 shows the five-parameter joint-confidence contours for the emission line intensity and line energy at three levels of significance (near minimum, $\chi^2_{min} + 1$; 68 percent, $\chi^2_{min} + 6$; 99 percent, $\chi^2_{min} + 15.1$). Each contour is the projection of the maximum extent of the 5 dimensional surface onto the plane defined by these two parameters. The continuum model includes a break at 25 keV. Two cautions must be given concerning the significance of these contours. The low-energy values are restrained by the requirement that the FWHM of the line be less than its mean energy (E_0). This restriction was introduced to prevent the inclusion of unphysical models, where the line width is much greater than the mean energy, which could otherwise produce acceptable fits to our data. The other caution is that the lowest intensities correspond to a FWHM of the line approaching the bin size used in the fitting. Since our bin size is larger than the energy resolution, higher values of these limits could be achieved with a smaller bin size. Smaller bins would also result in noisier contours due to increased statistical fluctuations in the data being fit. The particular choice of energy bins does effect the detailed contours but does not materially alter their general shape and values. The elongated shape of these contours with their very flat minimum reflects the strong

coupling of the fit parameters for the line. This strong coupling causes the large statistical error limits derived for the fit parameters from the extremes of the 68 percent contour. It is clear that the range of acceptable parameters inside the elongated contours is much more constrained than a rectangle enclosing the extreme values of the contours. In this case, tests of consistency with other results should be based on a comparison of the actual contours.

Also shown in Figure 4 are the results of two measurements by the MPI/AIT group. The points are the fit values derived from an emission line model, and the error bars are the extremes of the 68 percent contour (Voges et al., 1982, Trümper et al., 1978). We conclude that the results of fits to our data are marginally consistent with the September 1977 measurement and inconsistent with the measurement of May 1976.

A significant contribution to the uncertainty in this comparison results from the model used in fitting the data. In order to achieve a more model-independent comparison of our results with those of the MPI/AIT group we have made difference spectra by subtracting the MPI/AIT photon spectra from our spectrum (Figure 5). To form this difference we have rebinned our data in energy bins identical to those used by the MPI/AIT group. No normalization of the spectra have been performed, but all of these spectra are in reasonable agreement for the low-energy continuum (< 40 keV). The error bars in the difference spectrum include only the statistical errors from the individual data points. Each data point has been plotted in the histogram as a number of standard deviations from zero, thus the significance of these differences can be directly evaluated. Both of these difference spectra show the same systematic fluctuations in the region from 50 to 70 keV. The intensity of the MPI/AIT spectrum in this region is significantly higher than ours (> 3σ)

during both of their flights. The May 1976 spectrum also shows a significant excess in the region from 100 to 120 keV. While these differences are statistically significant, the possibility of a systematic error producing this variation cannot be eliminated. In particular, the MPI/AIT spectra have been deconvolved using an emission line model. Because of their limited energy resolution, a different model can produce significant differences in the deconvolved spectrum. Final confirmation of this variation will only be possible by continued high-resolution measurements.

Table 3 is a summary of the hard X-ray measurements of Her X-1 which have reported a significant feature in the spectrum. All of the values in the table are for emission-line fits to the data. Detailed comparisons similar to those performed for the MPI/AIT results are difficult because of differences in the data analysis procedures in other measurements. For instance, the HEAO-A4 result gives only a pulse minus off-pulse spectrum which is not directly comparable to our pulse minus off-source spectrum. It is interesting to note, however, that if we ignore the potential systematic problems, our two spectra are completely consistent. (A small renormalization is necessary.) In general, the comparison with low-resolution experiments is subject to significant errors due to the model dependence of their deconvolution of the spectrum. Detailed determinations of the shape of the feature and confirmation of possible variation in the shape require high resolution measurements with more statistics.

V. DISCUSSION

What light can the results of this experiment shed on the cyclotron line model for the hard X-ray feature in the Her X-1 spectrum? It is theoretically difficult for a cyclotron line model to produce a narrow (FWHM < 10 keV)

feature. Our confirmation of the broad (FWHM > 7 keV for an emission line) nature of the feature by an experiment with fine energy resolution eliminates this difficulty. Conclusive confirmation of the cyclotron line model requires extension of the spectrum to higher energies, both to observe the continuum emission above the line and to search for higher harmonics. Similar information is required to distinguish between absorption and emission line models. Our present experiment does not have sufficient sensitivity at energies above the line to improve on previous observations. We must note, however, that our best fit emission line model requires a sharp break in the continuum spectrum at 25 keV, to a very steep exponential (E_0 < 5.9 keV). (The fact that this continuum is steeper than the values derived by previous experiments is probably another result of our fine energy resolution and does not necessarily imply any inconsistency in the continuum measured.) The absorption line model results in a much smoother continuum and provides a more economical explanation of the observed features in the spectrum. This model is, therefore, slightly preferred.

The cyclotron line model provides a ready explanation for variations in the mean energy of the feature on both long and short term time scales. Since the energy of the line is proportional to the magnetic field, such variation can be explained by changes of the position of the emitting region in the field of the neutron star. Such movement could be the result of changes in the accretion rate. It should be noted, however, that our results for the continuum spectrum below the feature are completely consistent with those of the MPI/AIT group, in both shape and intensity. One would expect a significant change in the accretion rate to effect the luminosity of the source. For more discussion of the signficance of this variation see Prantzos and Durouchoux (1983).

VI. CONCLUSIONS

The most significant result of this measurement is the confirmation of the presence of the hard X-ray feature in the spectrum of Her X-1 by a high resolution experiment. In this experiment the feature is fully resolved and is not consistent with a narrow line. The confirmation of the feature by this experiment, which has different systematic uncertainties than the low-resolution scintillator experiments of previous observations, increases our confidence more than can be quantified by a simple consideration of statistical signficance. Moreover, we conclude that there are statistically significant differences between our spectrum and the May 1976 spectrum of the MPI/AIT group. We do not observe a 120 keV second harmonic line, even though a line at the same strength as the May 1976 MPI/AIT feature would be of $> 3\ \sigma$ significance in our data (see Figure 5). The primary feature in our data is at lower energy than in the MPI/AIT result (May 1976 or September 1977). This is implied by a $> 3\ \sigma$ deficit in the difference of the energy spectra between 50 keV and 60 keV, and corresponds to a most probable energy for an emission line feature of 39 keV in our result versus 58 and 51 keV for the two MPI/AIT measurements. This comparison strongly suggests that the feature is time dependent. Further measurements by both experiments are highly desirable, since confirmation of this result in the observations of a single experiment would eliminate possible systematic errors as the origin of this difference. The existance of a time variation would place new constraints on models of the origin of the hard X-ray feature.

ACKNOWLEDGEMENTS

This experiment has benefited from professional technical support from many people. Especially significant have been the contributions of H. Costlow and S. Brown for their work on the system hardware and participation in many long and difficult balloon-flight expeditions. Essential software support was provided by D. Argo, H. Eisericke and N. Laubenthal. We acknowledge the gracious help of Dr. J. Trümper in providing us with data from the MPI/AIT experiment for comparison to ours, and for his frank and open discussion of these results.

PRESENT ADDRESSES

T. L. Cline, B. J. Teegarden, and J. Tueller: Code 661,
Laboratory for High Energy Astrophysics, NASA/Goddard Space Flight Center,
Greenbelt, MD 20771, U.S.A.

W. S. Paciesas: Department of Physics, University of Alabama in Huntsville,
Huntsville, AL 35899, U.S.A.

D. Boclet, Ph. Durouchoux, J. M. Hameury and N. Prantzos: CEN-Saclay,
DPhG/SAP, 91191 Gif-sur-Yvette, CEDEX, France

R. C. Haymes, Department of Space Physics and Astronomy, Rice University,
Houston, TX 77001, U.S.A.

REFERENCES

Bahcall, J. N., and Bahcall, N. A., 1972 IAU Circ., Nos 2427 and 2428.

Bevington, P.R. 1969, Data Reduction and Error Analysis for the Physical Sciences (New York: McGraw-Hill).

Deeter, J. E., Boynton, P. E., and Pravdo, S. H. 1981, Ap. J., 247, 1003.

Gruber, D. E., Matteson, J. L., Nolan, P. L., Knight, F. K., Baity, W. A., Rothschild, R. E., Peterson, L. E., Hoffman, J. A., Sheepmaker, A., Wheaton, W. A., Primini, F. A., Levine, A. M., and Lewin, W. H. G. 1980, Ap. J. (Letters), 240, L127.

Lampton, M., Margon, B., and Bowyer, S. 1976, Ap. J., 208, 177.

Liller, W. 1972, IAU Circ., Nos 2415 and 2427.

McCray, R. A, Shull, J. M., Boynton, P. E., Deeter, J. E., Holt, S. S., and White, N. E. 1982, Ap. J., 262, 301.

Mészáros, P., Harding, A. K., Kirk, J. G., and Galloway, D. J. 1983, Ap. J. (Letters), 266, L33.

Nagel, W. 1981a, Ap. J., 251, 278.

Nagel, W. 1981b, Ap. J., 251, 288.

Paciesas, W., Baker, R., Boclet, D., Brown, S., Cline, T., Costlow, H., Durouchoux, P., Ehrmann, C., Gehrels, N., Hameury, J. M., Haymes, R., Teegarden, B., and Tueller, J. 1983, in print NIM.

Prantzos, N., and Durouchoux, P., 1983, in print Astr. Ap..

Pravdo, S. H., Boldt, E. A., Holt, S. S., and Serlemitsos, P. J. 1977, Ap. J. (Letters), 216, L 23.

Pravdo S. H., Bussard, R. W., Becher, R. H., Boldt, E. A., Holt, S. S., and Serlemitsos, P. J. 1978, Ap. J., 225, 988.

Sheepmaker, T., Jansen, F. A., Deerenberg, A. J. M., Ricker, G. R.,

Ballintine, J. E., Vallerga, J. V., and Lewin, W. H. G. 1981, Space Sci. Rev., 30, 325.

Staubert, R., Kendziorra, E., Pietsch, W., Proctor, R. J., Reppin, C., Steinle, H., Trümper, J., and Voges, W. 1981, Space Sci. Rev., 30, 311.

Tannenbaum, H., Gursky, H., Kellogg, E. M., Levinson, R., Schreier, E., and Giacconi, R. 1972, Ap. J. (Letters), 174, L143.

Trümper, J., Pietsch, W.. Reppin, C., Voges, W., Staubert, R., and Kendziorra, E. 1978, Ap. J. (Letters), 219, L105.

Tueller, J., Cline, T., Paciesas, W., Teegarden, B., Boclet, D., Durouchoux, P., Hameury, J., and Haynes, R. 1981, Proc. 17th Internat. Cosmic Ray Conf., Paris, 1, 95.

Ubertini, P., Bazzano, A., LaPadula, C. D., Polcaro, V. F., Manchanda, R. K., and Damle, S. V. 1981, Proc. 17th Internat. Cosmic Ray Conf., Paris, 1, 99.

Voges, W., Pietsch, W., Reppin, C., Trümper, J., Kendziorra, E. and Staubert, R. 1982, Ap. J., 263, 803.

TABLE 1

Spectral Fit Models

Model forms:

continuum only	$f(E) = f_c(E)$
emission line	$f(E) = f_c(E) + f_L^{+} \cdot G(E)$
absorption line	$f(E) = f_c(E) / [1 + E_W^{\neq} \cdot G(E)]$

Continuum flux:

power law, $f_c(E;\ I_0^{*},\ \gamma) = I_0 \cdot (20^{\gamma}) \cdot E^{-\gamma **}$

exponential, $f_c(E;\ I_0,\ E_0) = I_0 \cdot [20/\exp(-20/E_0)] \cdot \exp(-E/E_0^{\ddagger})/E$

power law with exponential cutoff,

$E < 25$ keV $\quad f_c(E;\ I_0) = I_0 \cdot E^{-1.2}$

$E > 25$ keV $\quad f_c(E;\ I_0,\ E_0) = I_0 \cdot [25^{-1.2} \cdot 25/\exp(-25/E_0)] \cdot \exp(-E/E_0)/E$

Line profile:

$G(E;\ E_m^{\neq\neq},\ FWHM) = 0.94 \cdot \exp(-2.76 \cdot [(E-E_m)/FWHM]^2)/FWHM$

* I_0 = spectrum normalization factor (I_0 normalized at 20 keV for the power-law and exponential continuum, I_0 normalized at 1 keV with a break at 25 keV for power law with exponential cutoff)

** γ = power-law spectral index

‡ E_0 = characteristic energy of exponential spectrum

‡‡ E_m = peak energy of Gaussian line profile

\+ f_L = total flux of emission line

^ E_W = equivalent width of absorption line

TABLE 2

Best Fit Parameters

Model	I_0 (ph/cm^2·s·keV)	γ (keV)	E_0 (ph/cm^2·s)	f_L (keV)	E_W (keV)	E_m (keV)	FWHM	χ^2	d.o.f.
power law	$6.0^{+1.0}_{-0.9} \cdot 10^{-3}$	$4.96^{+0.37}_{-0.36}$						31.8	18
exponential	$4.6^{+0.9}_{-0.8} \cdot 10^{-3}$		$7.95^{+1.22}_{-0.99}$					41.9	18
absorption line and exponential	$5.1^{+1.7}_{-1.3} \cdot 10^{-3}$		$9.86^{+1.77}_{-1.50}$		$14.5^{+13.8}_{-8.5}$	$35.4^{+2.3}_{-1.9}$	$8.4^{+5.3}_{-3.5}$	11.2	15
emission line and exponential	$6.2^{+1.2*}_{-1.7} \cdot 10^{-3}$		$6.08^{+1.58}_{-1.28*}$	$1.5^{+4.3*}_{-0.9} \cdot 10^{-3}$		$45.4^{+5.9}_{-12.0*}$	$9.3^{+31.9*}_{-5.3}$	19.9	15
emission line and power law with exponential cutoff[+]	$.142^{+.033*}_{-.035}$		$3.55^{+2.32}_{-1.81*}$	$4.7^{+5.9*}_{-3.5} \cdot 10^{-3}$		$38.6^{+9.1}_{-12.4*}$	$26.5^{+20.6*}_{-20.0}$	11.7	15

[+] Cutoff at 25 keV, I_0 normalized at 1 keV

* Line FWHM constrained to be < line energy (E_m)

TABLE 3

Her X-1 Emission Line Measurements

Date	Group	Intensity (f_L) (10^{-3} ph/cm^2·s)	Mean Energy (E_m) (keV)	Width (FWHM) (keV)
May 1976	MPI/AIT[1]	$3.4^{+2.0}_{-1.7}$	58 ± 5	11^{+26}_{-11}
Sept 1977	MPI/AIT[2]	2.7 ± 0.6	51.2 ± 2.8	21^{+9}_{-7}
Feb & Aug 1978	HEAO A-4[3]	5.5 ± 1.7	48 ± 4	28 ± 7
Apr 1980	Frascati[4]	2.1 ± 2.0	54 ± 6	11^{+14}_{-11}
May 1980	MIT/Leiden[5]	1.8 ± 0.4	$49.5^{+1.5}_{-3.0}$	18^{+6}_{-3}
Sept 1980	GSFC/CEN[6]	$4.7^{+5.9}_{-3.5}$	39^{+9}_{-12}	27^{+21}_{-20}

1 Trümper et al. (1978)
2 Voges et al. (1982)
3 Gruber et al. (1980)
4 Ubertini et al. (1981)
5 Sheepmaker et al. (1981)
6 This experiment

FIGURE CAPTIONS

Figure 1. HER X-1 light curve in the energy range 20 keV to 65 keV. The data have been plotted twice to aid the viewer. The dashed line represents the average background level.

Figure 2. The solid curve is the 3 sigma upper limit for a narrow line (1.4 keV FWHM). The data points are derived from broad line (> 10 keV FWHM) fits of the feature by Trümper et al. (1978), Voges et al. (1982), and this experiment. It is clear that these features cannot be attributed to a narrow emission line.

Figure 3. Data points are the photon spectrum derived by subtracting the off-source data from the data in the phase region labeled "PULSE" in Figure 1. Above 70 keV, the points are consistent with no source counts and are plotted as 2 sigma upper limits. The solid histogram is the uncorrected counts spectrum observed at the detector. It shows the same features that are apparent in the corrected spectrum.

Figure 4. Five parameter joint confidence contours for the emission line model parameters of intensity and mean (peak) energy. $\chi^2_{min} + 6$ corresponds to the 1 sigma (68 percent) confidence limit and $\chi^2_{min} + 15$ corresponds to the 99 percent confidence limit. Although the feature is of roughly the same statistical significance as the May 1976 result of the MPI/AIT group, the differences in the measured spectra result in much larger uncertainties on the emission line parameters derived from our spectrum.

Figure 5. Direct comparison of our results with the results of the MPI/AIT group. The difference between our results (September 1980) and the results of the MPI/AIT group (May 1976 and September 1977) are displayed

in units of standard deviations. In both comparisons there is a signfiicant (> 3σ) excess in the region from 50 to 60 keV in the MPI/AIT results over our spectrum. There is also a significant excess in the May 1976 spectrum in the region from 100 to 120 keV.

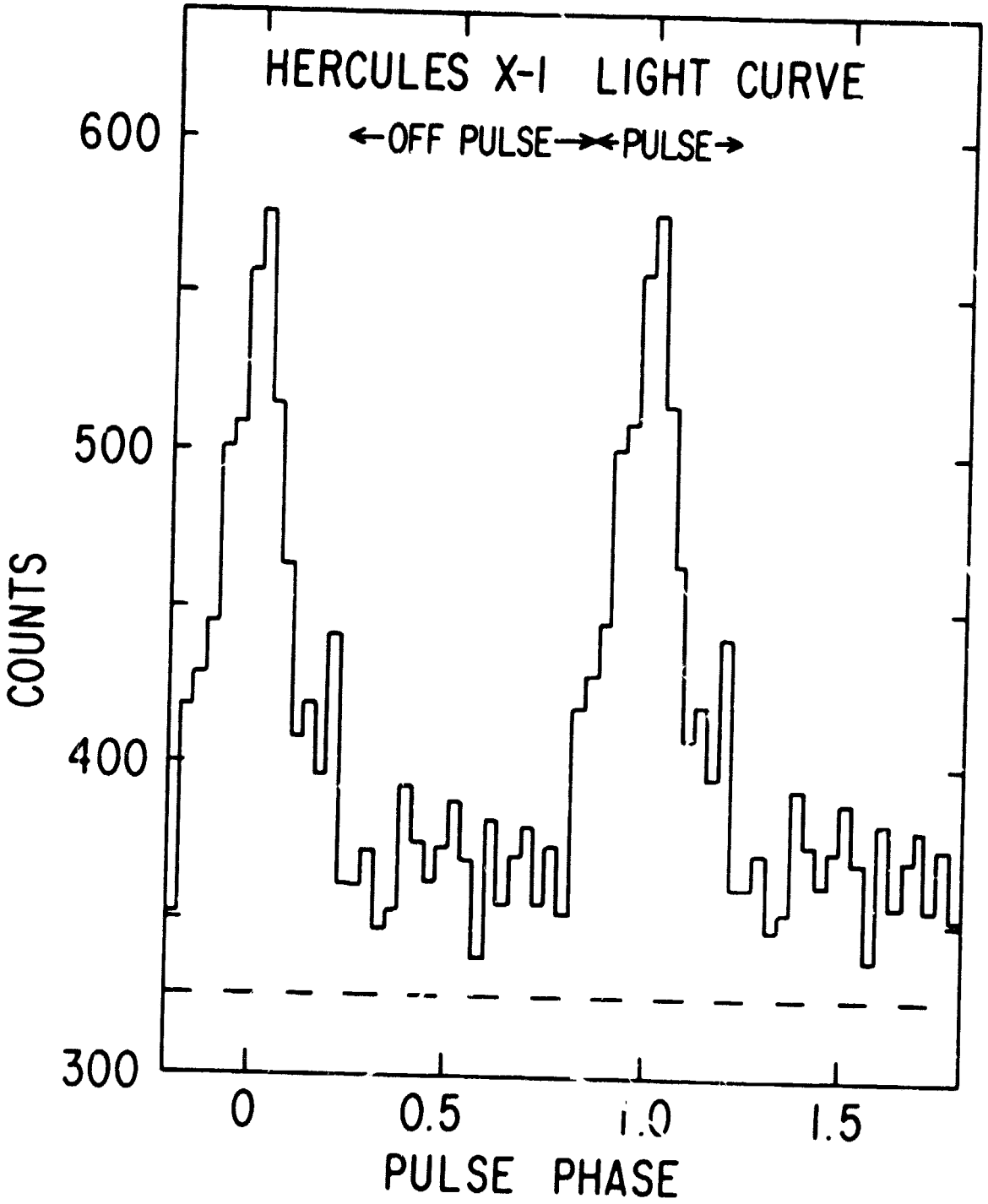

Figure 1

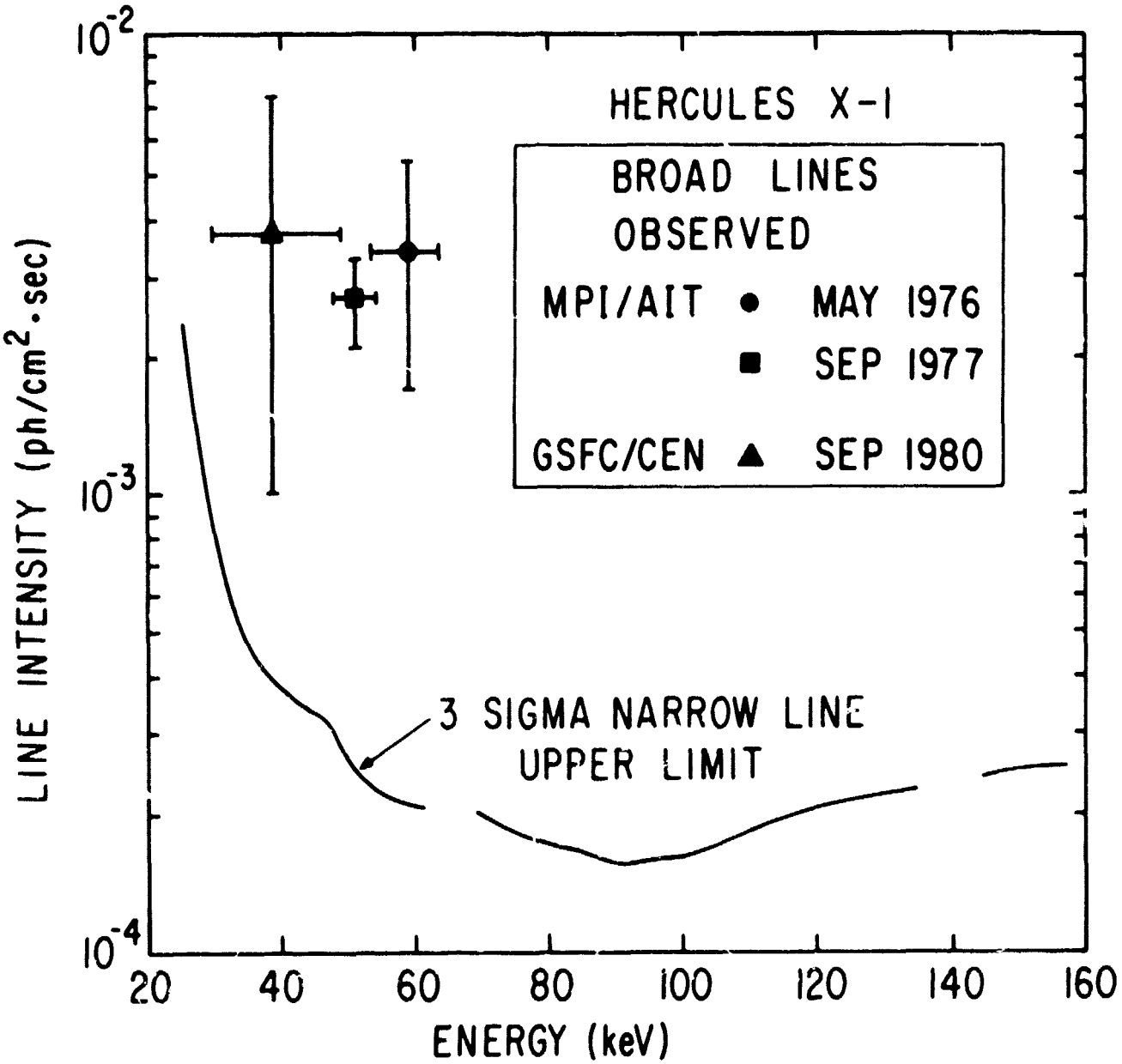

Figure 2

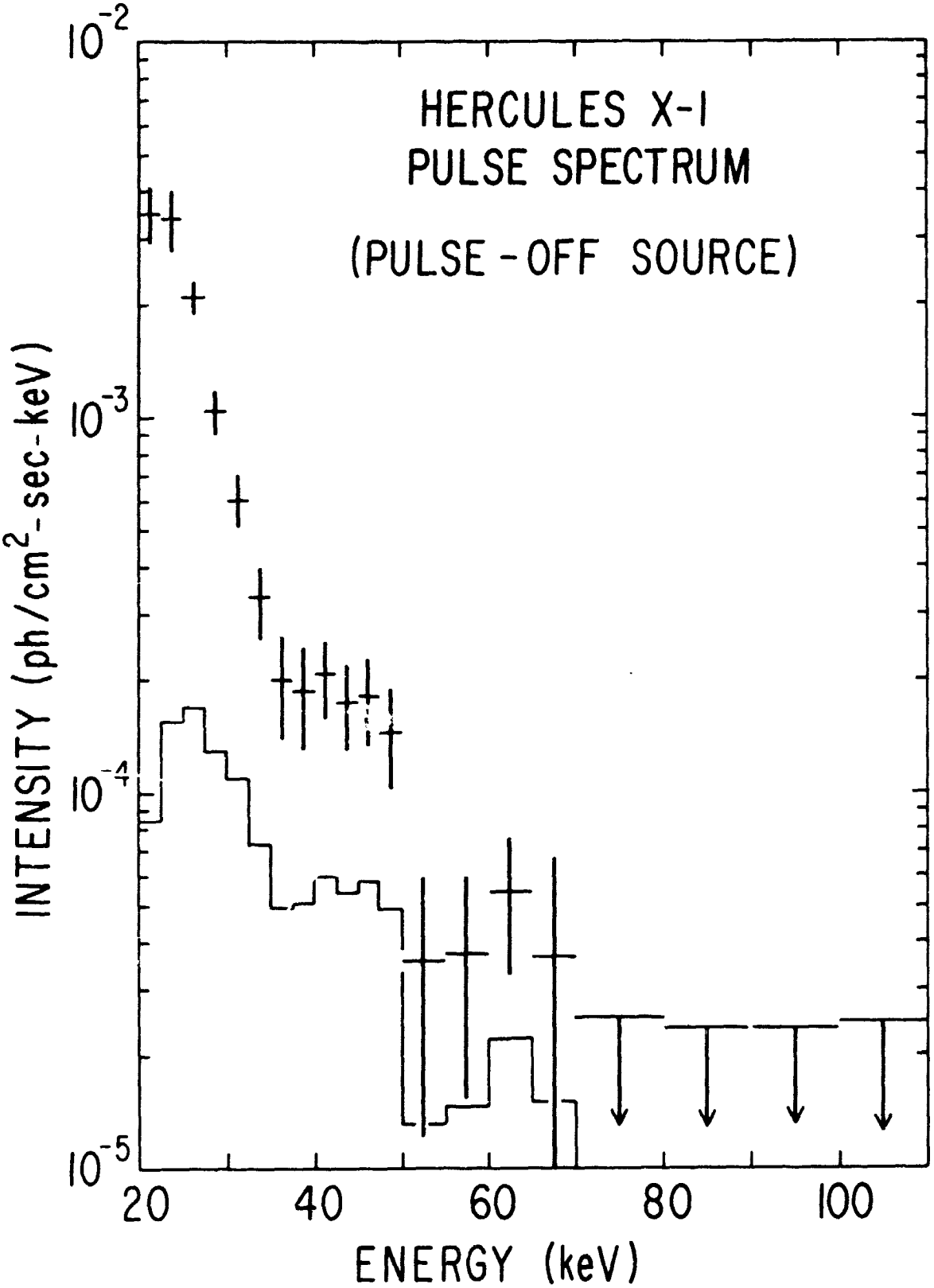

Figure 3

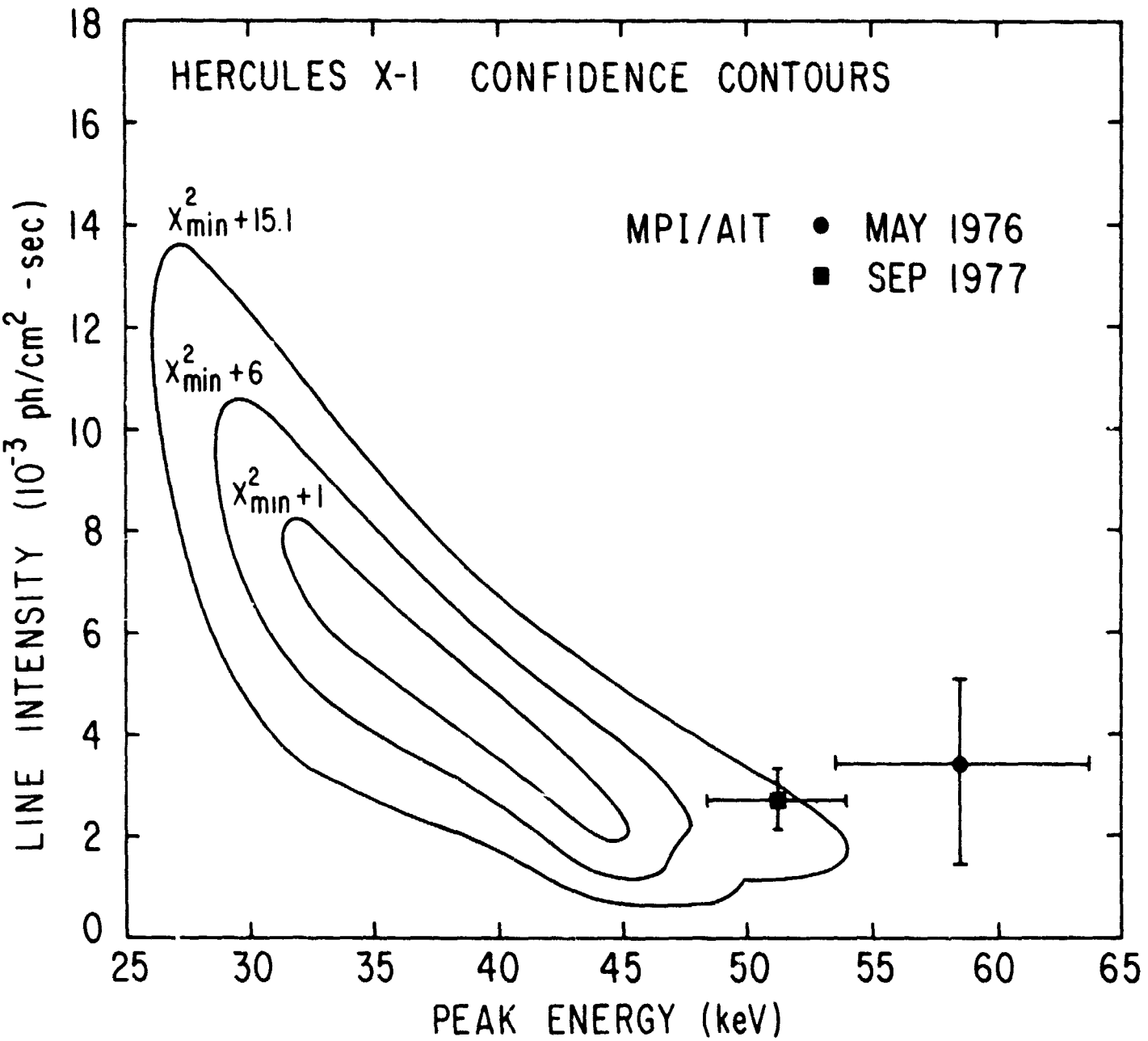

Figure 4

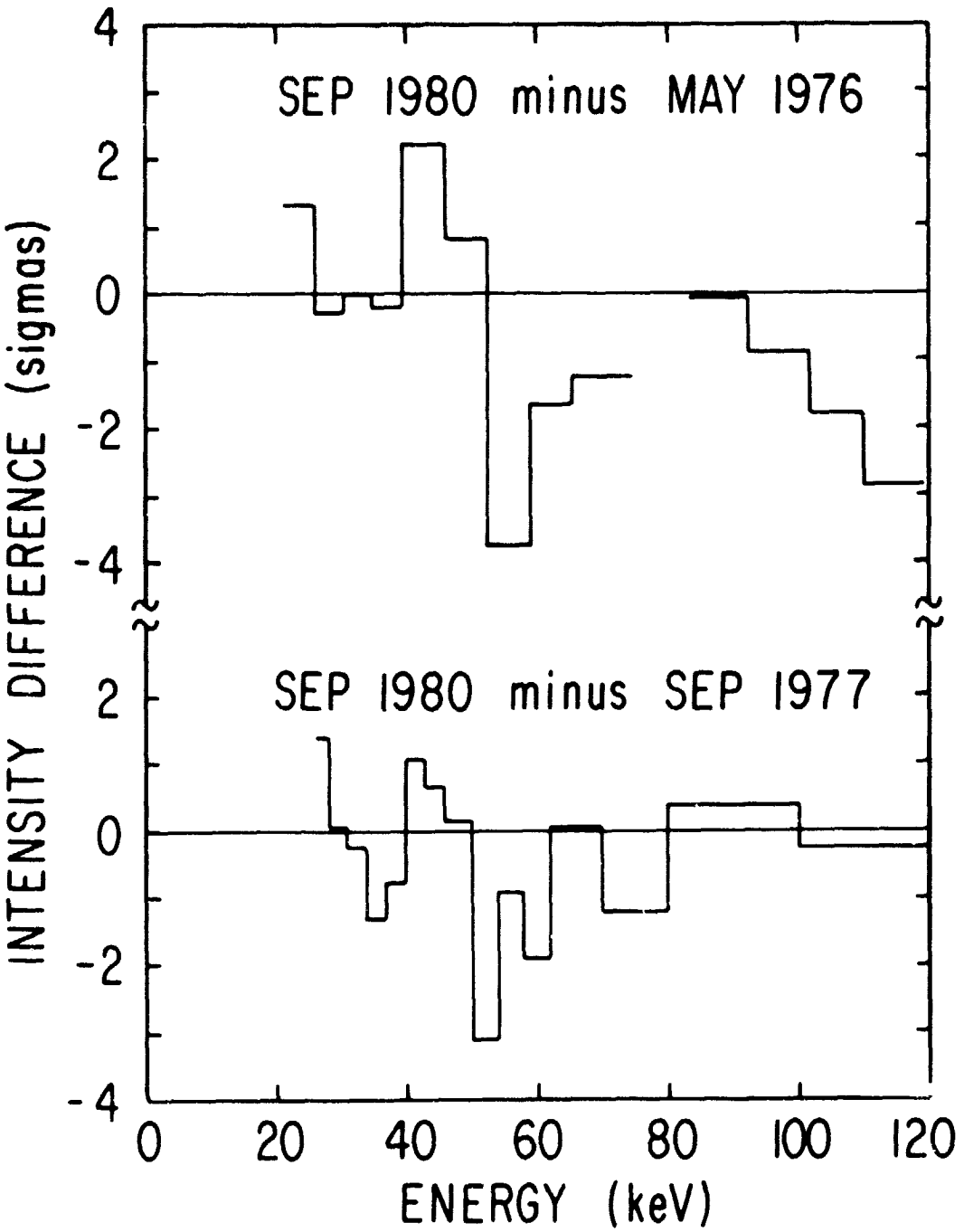

Figure 5